Temporal Regulation of Apoptotic and Anti-apoptotic Molecules After Middle Cerebral Artery Occlusion Followed by Reperfusion

**Bharath Chelluboina · Jeffrey D. Klopfenstein · Meena Gujrati ·
Jasti S. Rao · Krishna Kumar Veeravalli**

Abstract A tremendous effort has been expended to elucidate the role of apoptotic molecules in ischemia. However, many agents that target apoptosis, despite their proven efficacy in animal models, have failed to translate that efficacy and specificity in clinical settings. Therefore, comprehensive knowledge of apoptotic mechanisms involving key apoptotic regulatory molecules and the temporal expression profiles of various apoptotic molecules after cerebral ischemia may provide insight for the development of better therapeutic strategies aimed at cerebral ischemia. The present study investigates the extent of apoptosis and the regulation of apoptotic molecules both at mRNA and protein levels at various time points after focal cerebral ischemia in a rat model of middle cerebral artery occlusion. In this study, we performed various techniques, such as TTC (2,3,5-triphenyltetrazolium chloride), H&E (hematoxylin and eosin), and TUNEL (terminal deoxy nucleotidyl transferase-mediated nick-end labeling) staining, along with polymerase chain reaction (PCR) microarray, antibody microarray, reverse transcription (RT)-PCR, immunofluorescence, and immunoblot analyses. Our research provided a large list of pro-apoptotic and anti-apoptotic molecules and their temporal expression profiles both at the mRNA and protein levels. This information could be very useful for designing future stroke therapies and aid in targeting the right molecules at critical time to obtain maximum therapeutic benefit.

B. Chelluboina · J. S. Rao · K. K. Veeravalli (✉)
Department of Cancer Biology and Pharmacology, University of Illinois College of Medicine at Peoria, One Illini Drive, Peoria, IL 61605, USA
e-mail: krishnav@uic.edu

J. D. Klopfenstein · J. S. Rao
Department of Neurosurgery, University of Illinois College of Medicine at Peoria, Peoria, IL 61605, USA

M. Gujrati
Department of Pathology, University of Illinois College of Medicine at Peoria, Peoria, IL 61605, USA

Introduction

Despite decades of work, no clinically effective therapies exist to facilitate recovery from stroke. Globally, of the 15 million people who suffer a stroke each year, more than 5 million die and a further 5 million are left permanently disabled [1]. Emotional and behavioral changes after stroke can be distressing to survivors and family members alike. Current treatment options offer only modest benefits, creating a pressing need for new and effective treatments.

There is overwhelming evidence to suggest that both necrosis and apoptosis contribute significantly to cell death subsequent to cerebral ischemia. After focal cerebral ischemia, most of the cells in the ischemic core undergo necrosis and the cell death in the ischemic penumbra is considered an active process that leads to apoptosis [2]. In the early stages of cerebral infarction, neurons in the ischemic core display several characteristics of early apoptosis, which include cytoplasmic and nuclear condensations and activation-specific caspase-cascades [3].

Although there is a clear indication of initiation of the apoptotic pathway in the ischemic core, the complete morphological changes of apoptosis are not observed at the end stages of infarction. Termination of the apoptotic process in the ischemic core could be due to severe energy level impairment that may cause a shift from apoptosis toward secondary necrosis [4]. The activated caspases or calpains eventually cleave ion pumps, such as plasma membrane Ca^{2+} pump and Na^+/Ca^{2+} exchanger, which results in the disruption of calcium homeostasis that can finally switch apoptotic signaling to necrosis [5, 6]. Necrosis is a more complex phenomenon that, while linked to apoptosis, has a separate,

significant role in cerebral ischemia. In contrast, in the ischemic penumbra, energy-dependent caspase-activation cascades have been observed where apoptosis can fully develop because of the residual blood supply.

Therapies targeting cell death in the ischemic core likely will be less successful than those targeting cell deaths in the penumbra. This could be the major reason for the clinical failure of many drugs that are aimed at excitotoxicity and oxidative stress. Targeting apoptosis, which plays a key role both in the ischemic core and in the penumbra, could offer a significant therapeutic benefit. Both extrinsic and intrinsic apoptotic pathways play vital roles, and upon initiation these pathways recruit downstream apoptotic molecules to execute cell death cascades. Each of these pathways contains both caspase-dependent and caspase-independent components.

A tremendous effort has been made to elucidate the role of apoptotic molecules after cerebral ischemia. Several agents targeting caspases and Bcl-2 family members demonstrated efficacy in animal models of cerebral ischemia [7–14]. IDN-6556 is a broad-spectrum caspase inhibitor and when administered to humans during liver transplantation, offered local therapeutic protection against cold ischemia/warm reperfusion-mediated apoptosis and injury [15]. Any approach targeting a single molecule/mechanism may not provide the desired therapeutic benefit due to the complex pathology of ischemic stroke. Moreover, because of the apoptotic cross-talk among several pathways, inhibition of one apoptotic pathway may augment an alternative one.

It is vital that optimal neuroprotective approaches to treat cerebral ischemia include combination treatment strategies. Therefore, comprehensive knowledge of apoptotic mechanisms involving key apoptotic regulatory molecules and the temporal expression profile of various apoptotic molecules after cerebral ischemia may provide insight for the development of better therapeutic strategies aiming at cerebral ischemia. Hence, in the present study, we aimed to investigate the extent of apoptosis and the regulation of apoptotic molecules both at the mRNA and protein levels at various time points after focal cerebral ischemia in a rat model of middle cerebral artery occlusion (MCAO).

Methods

The Institutional Animal Care and Use Committee (IACUC) of the University of Illinois College of Medicine at Peoria approved all surgical interventions and post-operative animal care.

Animals

In this study, we used male Sprague–Dawley rats. All animal experiments were conducted in accordance with the IACUC guidelines. Adult male Sprague–Dawley rats weighing 230–

250 g were procured from Harlan Laboratories (USA). Animals were housed in a 12-h light/dark cycle at a controlled temperature and humidity with free access to food and water. Animals were randomly assigned to groups, and each group consisted of at least 20 animals. After the animals reached a weight of 260 ± 5 g, they were subjected to an MCAO procedure followed by their sacrifice at various time points. Study design, group description, and the number of animals used for various experiments are included in Table 1. All the procedures that were performed on the animals were in compliance with the approved IACUC protocol.

Antibodies

Anti-Fas, anti-TNFR1, anti-TNFR2, anti-ERK1, anti-phospho-ERK, anti-caspase-3, anti-XIAP, anti-cytochrome c, anti-Smac, anti-Bcl2, and anti-bax antibodies were obtained from Santa Cruz Biotechnology (Santa Cruz, CA). Anti-Akt, anti-Bad, anti-AIF, and anti-cleaved caspase-3 antibodies were obtained from Cell Signaling Technology (Danvers, MA). Anti-NeuN antibody was obtained from Millipore (Billerica, MA). Glyceraldehyde-3-phosphate dehydrogenase (GAPDH) antibody was obtained from Novus Biologicals (Littleton, CO).

Experimental MCAO Model

After the animal reached a weight of 260 ± 5 g, it was subjected to MCAO procedure. Anesthesia was induced and maintained during the surgical procedure with isoflurane (0.5–3 %). A heating pad and a heating lamp were used to maintain the rectal temperature between $37\pm5°C$. A ventral midline incision (~25 mm) was made in the neck and the right common carotid, internal carotid and external carotid arteries were surgically exposed. Two loose ligatures (5–0 silk suture) were then placed around the external carotid artery. The external carotid artery was permanently ligated rostral with one ligature. A microaneurysm clip was applied to the external carotid artery near its bifurcation with the internal carotid artery. A small puncture opening was made in the external carotid artery. The pre-determined optimal inserted length on the bare surface of the intraluminal suture (monofilament) material of appropriate size to the weight range of animals used (Doccol Corporation, California) was marked. Monofilament was inserted through the opening and the other loose ligature was tightened around the lumen containing the monofilament. The knot should be readily undone, yet tight enough to stop bleeding. The microaneurysm clip was removed from the external carotid artery and the monofilament was then gently advanced from the lumen of the external carotid artery into the internal carotid artery for a distance of ~19 to 20 mm beyond the bifurcation of the common carotid artery. Skin on the neck incision was closed with surgical wound clips. Animals were maintained

Table 1 Description of experimental groups

Group no.	Group description	Designation	Number of animals studied			
			TTC staining	IHC (IF/TUNEL/H&E staining)	Immunoblot/RT-PCR/ Microarray	Total
1	Animals subjected to the MCAO procedure without monofilament insertion	Sham control	3 (PSD1) 3 (PSD7)	3 (PSD7)	3 (PSD7)	12
2	Animals subjected to the MCAO procedure with 1 h monofilament insertion	1 h ischemia-induced	4 (PSD1)	–	–	4
3	Animals subjected to the MCAO procedure with 2 h monofilament insertion	2 h ischemia-induced	3 (PSD1) 5 (PSD7)	3 (PSD1) 3 (PSD3) 4 (PSD5) 4 (PSD7)	3 (PSD1) 4 (PSD3) 3 (PSD5) 5 (PSD7)	37

TTC 2,3,5-triphenyltetrazolium chloride, *IHC* immunohistochemistry, *TUNEL* terminal deoxy nucleotidyl transferase-mediated nick labeling, *H&E* hematoxylin and eosin, *RT-PCR* reverse transcriptase polymerase chain reaction, *MCAO* middle cerebral artery occlusion, *PSD1* sacrificed 1 day post-MCAO procedure, *PSD3* sacrificed 3 days post-MCAO procedure, *PSD5* sacrificed 5 days post-MCAO procedure, *PSD7* sacrificed 7 days post-MCAO procedure

in this state (induction of cerebral ischemia) for 1 or 2 h. To restore the blood flow 1 or 2 h after MCA occlusion, the surgical site was re-opened by removing the wound clips. The microaneurysm clip was removed, the knot was loosened, the monofilament was withdrawn and the knot was re-tied to stop bleeding. This procedure initiated reperfusion. The skin was sutured to close the neck incision and the rats were allowed to recover. Animals subjected to the MCAO procedure were treated with appropriate doses of analgesics and antibiotics as mentioned in the IACUC protocol. Post-MCAO procedure, the animals were sacrificed at various time points (post-surgery day 1 [PSD1], PSD3, PSD5, or PSD7). The brain tissues obtained from these animals were utilized for various experimental procedures.

TTC Staining and Measurement of Infarct Size

At various time points after the MCAO procedure (PSD1, PSD3, PSD5 or PSD7), animals from various groups allocated for 2,3,5-triphenyltetrazolium chloride (TTC; Sigma) staining procedure were deeply anesthetized with pentobarbital and then decapitated. Brains were then removed rapidly and placed in an adult rat brain matrix (Kent Scientific Corporation) that was pre-chilled. Matrix containing the brain tissue was then placed in a freezer at −70 °C for 5–8 min and sliced into 2-mm-thick coronal sections. These slices were stained in 2 % TTC for 30 min at 37 °C in the dark. The infarction area and hemisphere area of each section was traced and measured using Image J analysis software (NIH). The infarct size was quantified by using the formula, infarct volume={(volume of contralateral hemisphere)−(volume of non-ischemic ipsilateral hemisphere)}/volume of contralateral hemisphere. This formula accounts for the possible interference of brain edema on infarct volume.

Brain Tissue Fixation and Sectioning

Under deep anesthesia with pentobarbital, rats were sacrificed at various intervals post-MCAO procedure (PSD1, PSD3, PSD5 or PSD7) for hematoxylin and eosin (H&E) staining, terminal deoxy nucleotidyl transferase-mediated nick labeling (TUNEL) assay, and immunofluorescence analysis. Briefly, animals were perfused through the left ventricle with 70–100 ml of phosphate buffered saline (PBS), followed by 100–150 ml of 10 % buffered formalin phosphate (Fisher Scientific, New Jersey). The brains of the animals from various treatment groups and sham controls were then removed, fixed in 10 % buffered formalin, and embedded in paraffin. Serial coronal brain sections were cut at a thickness of 5 μm with a microtome.

Hematoxylin and Eosin Staining

Paraffin-embedded brain sections of various groups of animals including sham controls were de-paraffinized, rehydrated and then subjected to H&E staining according to a standard protocol. H&E-stained sections were coverslipped and observed under a light microscope. All the slides were evaluated by a neuropathologist blinded to the treatments.

Terminal Deoxy Nucleotidyl Transferase-Mediated Nick-End Labeling Assay

The extent of apoptosis in the paraffin-embedded coronal brain sections of animals from all the groups was analyzed

Table 2 Rat specific apoptotic genes analyzed by RT-PCR at various time points after middle cerebral artery occlusion followed by reperfusion

Gene	Reference sequence	Primer sequence		Product size
		Forward (5′–3′)	Reverse (5′–3′)	
Fasl (CD95-L)	NM_012908	tgcctccactaagccctcta	aggctgtggttggtgaactc	166
TNF	NM_012675	agatgtggaactggcagagg	cccatttgggaacttctcct	178
Fas	NM_139194	ctggaatcccaagtcctgaa	tgataccagcactggagcag	214
TNFR1	NM_013091	accaagtgccacaaaggaac	ctggaaatgcgtctcactca	249
TNFR2	NM_130426	aaatgcaagcacagatgcag	cagcagacccagagttgtca	244
Bad	NM_022698	caggcagccaataacagtca	ccctcaaattcatcgctcat	209
Bid	NM_022684	accgtgatttccaccaagag	tggcaatgttgtggatgact	180
Bax	NM_017059	ctgcagaggatgattgctga	gatcagctcgggcactttag	174
Bcl2	NM_016993	cgactttgcagagatgtcca	atgccggttcaggtactcag	223
Birc4 (XIAP)	NM_022231	ggccagactatgcccattta	cgaagaagcagttgggaaag	171
Birc5 (Survivin)	NM_022274	cctaccgagaatgagcctga	acggtcagttcttccacctg	155
Cidea	NM_001170467	ctcggctgtctcaatgtcaa	ccgcataaaccaggaactgt	151
Cideb	NM_001108869	gacccttccgtgtctgtgat	ggcgatgtccttgctatgtt	239
Dffb (Cad)	NM_053362	gctcaagtccgtgcagtaca	ctgttgccatagggggttgat	153
Diablo (Smac)	NM_001008292	ctcggagcgtaacctttctg	tcctcatcagtgcttcgttg	195
Tnfrsf10b	NM_001108873	aaaccaggcagctttgaaga	agctgggttgtttccatttg	219
Tnfsf10 (Trail)	NM_145681	gcttcagtcagcacttcacg	gtcccaaaaatcccatctt	179
Naip2	XM_226742	gcatggagaattggaaggaa	cagactcctggcctcttgac	248
NF-kB	XM_342346	aggccattgaagtgatccag	cagtgagggactccgagaag	204
TP53 (p53)	NM_030989	tctccccagcaaaagaaaaa	cttcgggtagctggagtgag	168
Caspase 3	NM_012922	ggacctgtggacctgaaaaa	gcatgccatatcatcgtcag	159
Caspase 8	NM_022277	tgaaggagctgcttttccat	atcaagcaggctcgagttgt	239
Caspase 14	NM_001191776	tgcagaggagagcacagaga	gaacacatccgtcagggtct	192
β-Actin	NM_031144	gtcgtaccactggcattgtg	ctctcagctgtggtggtgaa	181

by TUNEL assay using In Situ Cell Death Detection Kit (Roche, Indianapolis, IN) according to the manufacturer's instructions. Briefly, the paraffin-embedded tissue sections were de-paraffinized, rehydrated, treated with proteinase K working solution, and permeabilized. Permeabilized tissue sections were incubated with the TUNEL reaction mixture in a humidified atmosphere for 60 min at 37 °C in the dark. Sections were counterstained for nuclei with DAPI (Dako, Carpinteria, CA), coverslipped using fluorescent mounting medium (Dako), and observed under a fluorescence microscope (Olympus IX71). The results were quantified by counting the number of TUNEL-positive cells in at least five different ischemic zones of ipsilateral brain region and non-ischemic contralateral brain regions of the tissue sections obtained from at least three animals per group.

Immunofluorescence Analysis

This technique was used to identify the changes in the expression of caspase-3 protein in rat brains in response to right MCAO. Paraffin-embedded brain sections of various groups of animals were de-paraffinized, subjected to antigen retrieval, permeabilized, processed with anti-caspase-3 primary antibody followed by Alexa Fluor® 488 (goat anti-rabbit IgG, green) fluorescent-labeled secondary antibody, counterstained with DAPI, coverslipped, and observed using a confocal microscope (Olympus Fluoview). Negative controls (without primary antibody or using isotype specific IgG) were maintained for all the samples. All the slides were evaluated by a neuropathologist blinded to the treatments. The results were quantified by counting the number of caspase-3-positive cells in at least five different ischemic zones of ipsilateral brain region and non-ischemic contralateral brain regions of the tissue sections obtained from at least three animals per group. To evaluate neuronal apoptosis, another set of paraffin-embedded brain sections from MCAO-subjected rats that were sacrificed 7 days post-MCAO (PSD7) were subjected to co-localization analysis with caspase-3 and NeuN antibodies followed by appropriate Alexa Fluor secondary antibodies.

RNA Extraction and cDNA Synthesis

Total RNA was extracted using TRIzol reagent (Invitrogen, Carlsbad, CA) from the ischemic ipsilateral brain regions of

Fig. 1 Effect of the duration of the occlusion and reperfusion period on infarct volume. **a** Representative TTC staining images of the rat coronal brain sections of sham-operated and MCAO (middle cerebral artery occlusion)-subjected rats sacrificed 1 day post-surgery (*PSD1*) and 7 days post-surgery (*PSD7*); $n \geq 3$. The *white-colored areas* represent the infarct regions in these sections, and the *red-colored areas* represent normal areas. **b** Quantification of infarct volume using image analysis software. The possible influence of edema on infarct volume was corrected by standard methods (volume of contralateral hemisphere−volume of non-ischemic ipsilateral hemisphere), with infarcted volume expressed as a percentage of the contralateral hemisphere. Values are expressed as mean±SEM; *$p < 0.05$
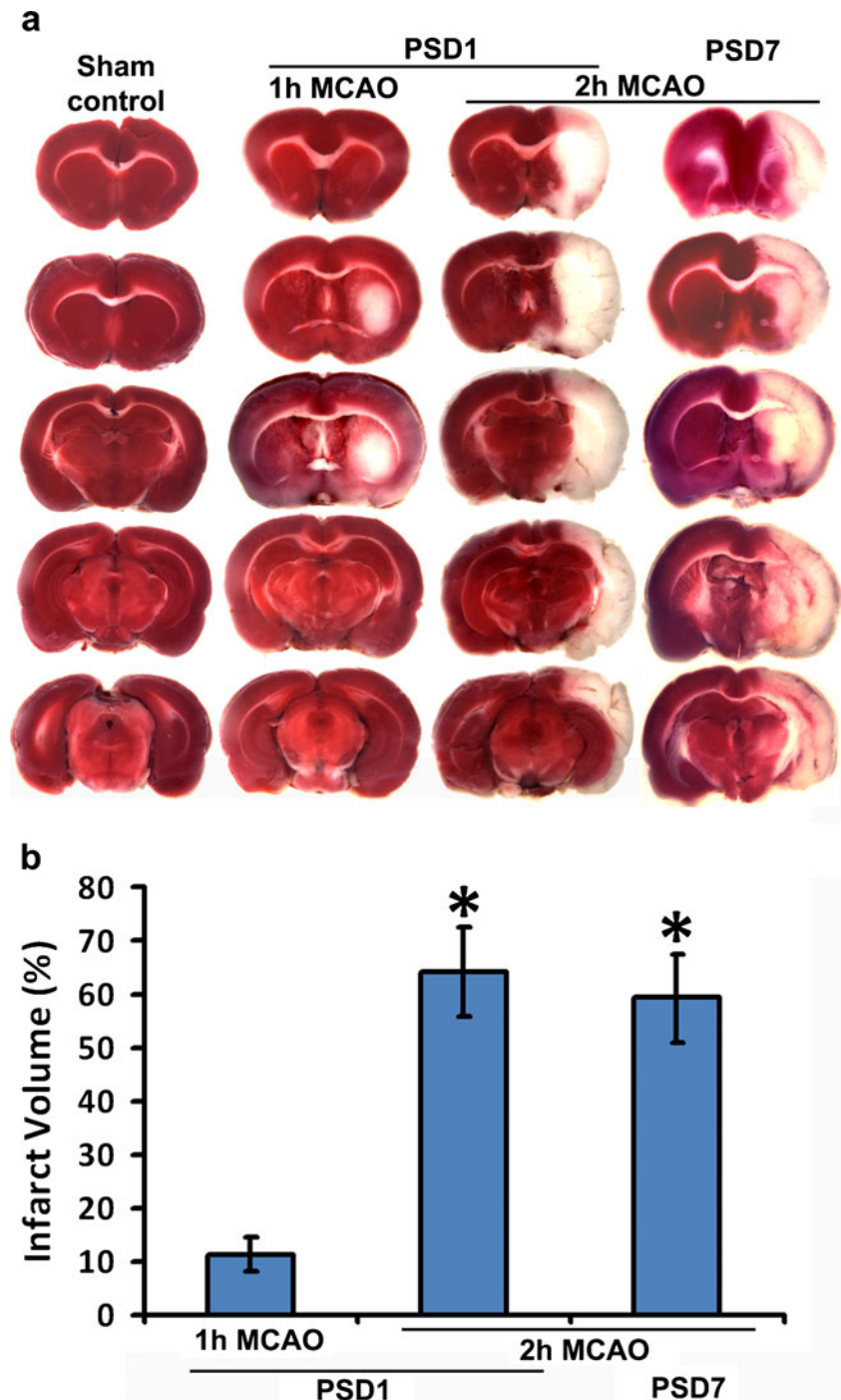
rats sacrificed at various time points after the MCAO procedure (PSD1, PSD3, PSD5, or PSD7) and sham controls. Briefly, total RNA was extracted with TRIzol and precipitated with isopropyl alcohol, washed in ethanol, and resuspended in RNase-free water. Then, 1 μg of total RNA was reverse transcribed into first-strand cDNA using the Transcriptor First Strand cDNA Synthesis Kit (Roche) according to the manufacturer's instructions. The cDNAs thus obtained were used for reverse transcription polymerase chain reaction (RT-PCR) analysis and rat apoptosis RT^2 Profiler PCR array.

Apoptosis PCR Array

We used the RT^2 Profiler Rat Apoptosis PCR Array (Catalog # PARN-012ZD; SA Biosciences) because of the advantages of RT-PCR performance combined with the ability of microarrays to detect the expression of many genes simultaneously. Each array contains a panel of 96 primer sets of 84 relevant apoptosis pathway focused genes, plus five housekeeping genes, and three RNA and PCR quality controls. The cDNAs obtained from the brain sections of sham

controls and the ischemic ipsilateral brain sections of MCAO-subjected rats sacrificed on day 1 and day 7 post-MCAO procedure were loaded onto microarray plates along with FastStart SYBR Green (Roche) according to the manufacturer's instructions. The sample-loaded microarray plate was subjected to real-time PCR analysis in iCycler IQ (Multi Color Real-Time PCR Detection System; Bio-Rad Laboratories, California). Real-time PCR was carried out under the following conditions: one cycle of 95 °C for 10 min, and 40 cycles of 95 °C for 15 s and 60 °C for 1 min. Data obtained in the form of C_t values was analyzed by using web-based analysis software (http://pcrdataanalysis.sabiosciences.com/pcr/arrayanalysis.php). Changes in gene expression were shown as a fold increased or decreased. The cut-off induction determining expression was ±2.0-fold changes, and the genes fitting these criteria were considered to be up-regulated or down-regulated, respectively. We performed the PCR microarray analysis on the samples obtained from three different animals per group.

RT-PCR Analysis and Agarose Gel Electrophoresis

RT-PCR analysis was performed using cDNAs obtained from the brains of various treatment groups, appropriate primer sets listed in Table 2, and GoTaq® Green Master Mix (Promega) as per the manufacturer's instructions. RT-PCR was set up in C1000 Touch Thermocycler (Bio-Rad Laboratories) using the following PCR cycle: (95 °C for 5 min [95 °C for 30 s, 58–62 °C for 30 s, and 72 °C for 30 s] × 40 cycles, and 72 °C for 10 min). The RT-PCR end product was resolved on a 1.6 % agarose gel, visualized, and photographed under UV light. The housekeeping gene β-actin was used to verify that similar amounts of cDNA were loaded in all the lanes.
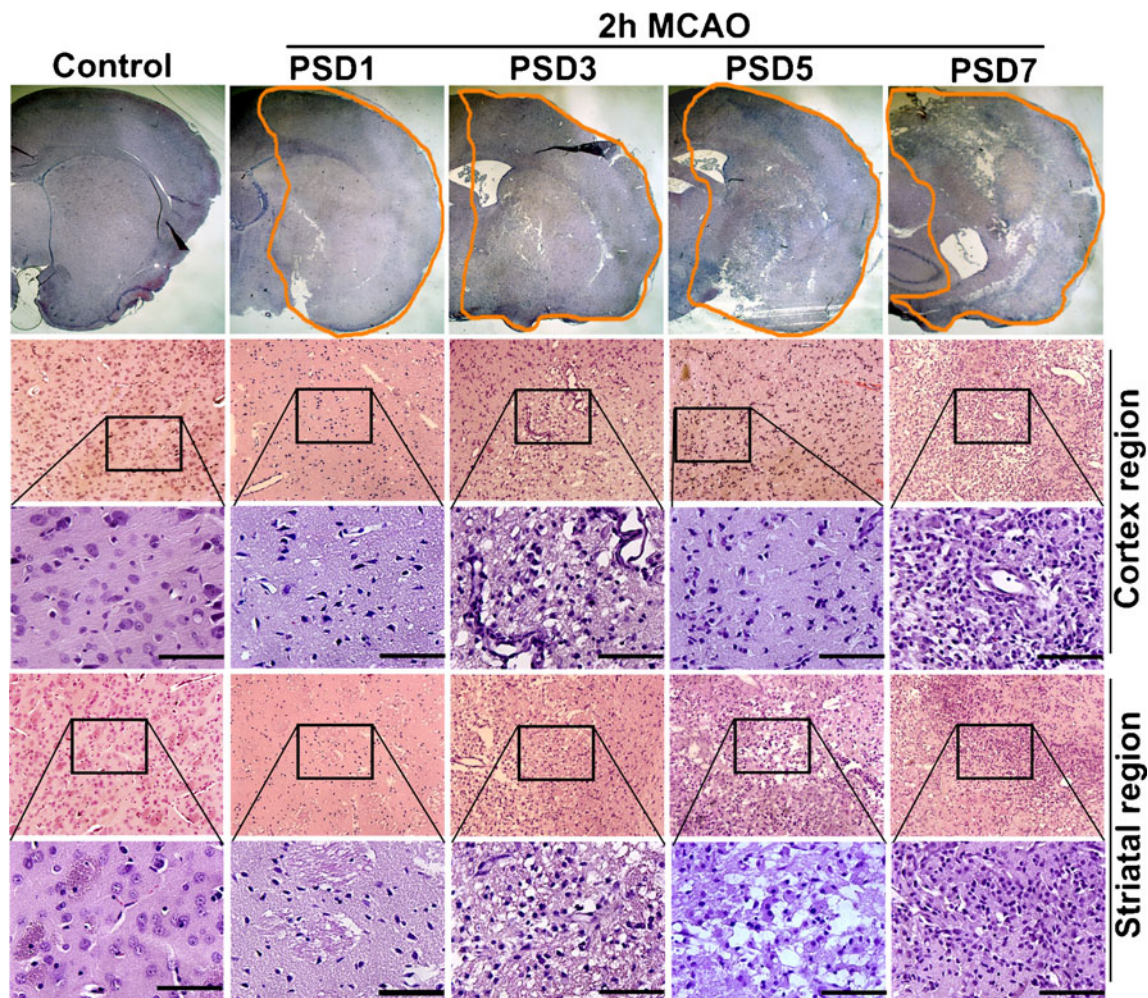
Fig. 2 Representative hematoxylin and eosin stained paraffin-embedded tissue sections from rat brains subjected to 2 h of middle cerebral artery occlusion (*MCAO*) followed by their sacrifice at various time points after MCAO; $n \geq 3$. The bordered area in the *top row* images indicates the damaged brain tissue. All the remaining are respective higher magnification images from the ischemic cortex and striatal regions showing interstitial edema and damaged neurons that have a condensed, irregular shaped and darkly stained nuclei which are absent in control brain sections. Scale bar=50 μm; PSD-post-surgery/MCAO day
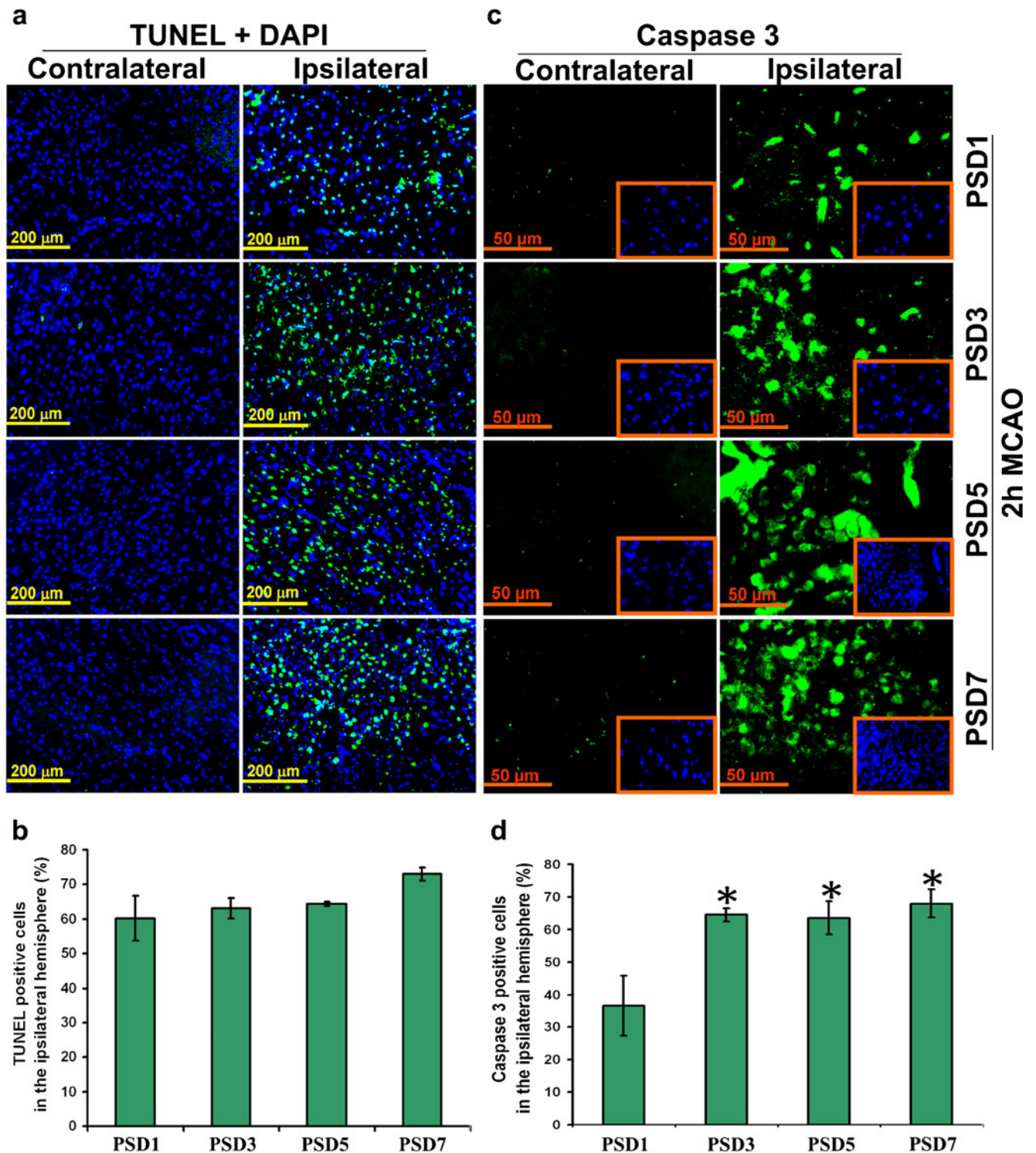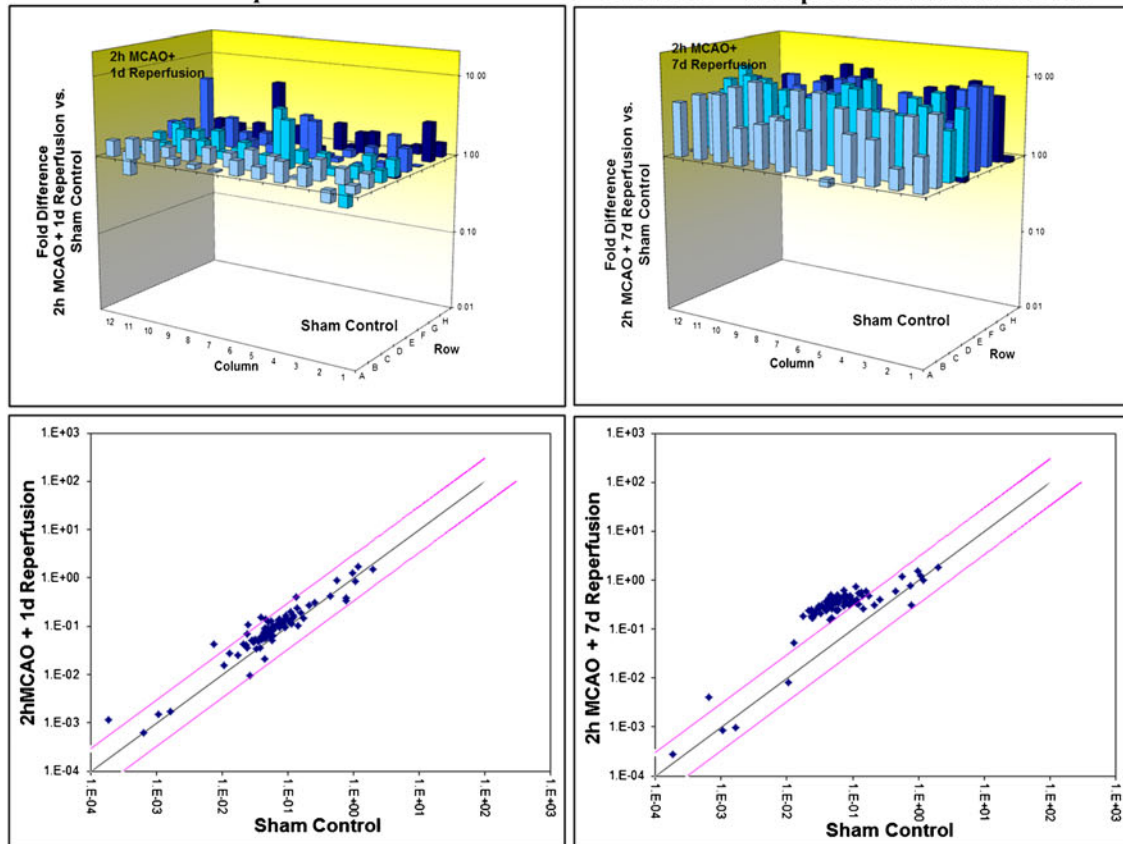
Fig. 3 Apoptosis after focal middle cerebral artery occlusion (*MCAO*) followed by reperfusion in rats. **a** TUNEL assay on the paraffin-embedded coronal brain sections of rats sacrificed at various time points after MCAO. Green fluorescence in the ipsilateral/ischemic brain regions of the representative images indicates TUNEL-positive cells. Blue fluorescence indicates DAPI staining of the nuclei. PSD is post-surgery/MCAO day. **b** Quantification of the TUNEL-positive cells in ipsilateral regions; $n \geq 3$. Values are expressed as mean±SEM. **c** Immunohistochemical analysis of caspase-3 expression in contralateral and ipsilateral rat brain coronal sections post-MCAO. Green fluorescence indicates caspase-3 protein expression. *Insets* show DAPI staining. **d** Quantification of caspase-3 protein expression in ipsilateral regions; $n \geq 3$. Values are expressed as mean±SEM; *$p < 0.05$ compared to PSD1
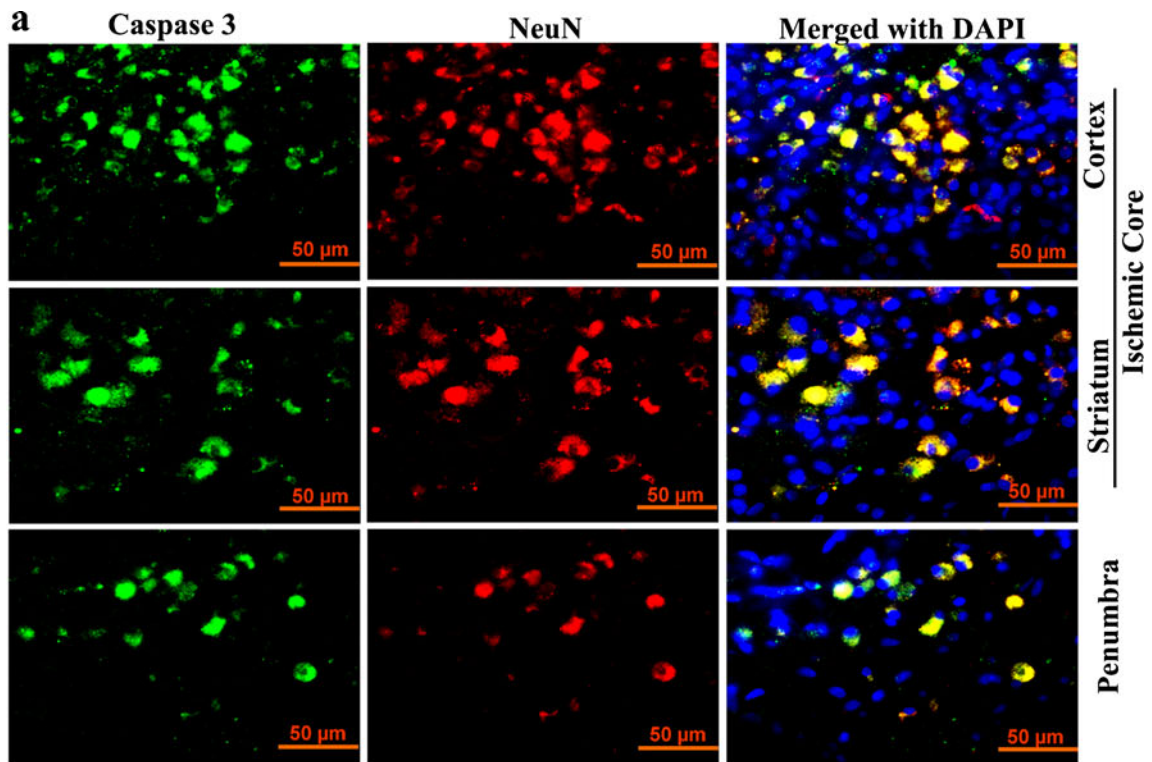
◀ **Fig. 4** Neuronal apoptosis and the regulation of apoptotic molecules at the mRNA level after focal middle cerebral artery occlusion (*MCAO*) in rats. **a** Immunofluorescence analysis showing the expression of caspase-3 (green fluorescence) and NeuN (red fluorescence) in cortex and striatal regions of the ischemic core and the penumbra in rats subjected 2 h of MCAO and sacrificed 7 days post-MCAO procedure. Yellow fluorescence indicates neuronal apoptosis. Nuclei were stained with DAPI. **b** PCR microarray analysis of rat apoptotic genes from the cDNAs obtained from the ischemic region of MCAO-subjected rats and from sham controls. Total RNA was extracted from the tissues, reverse-transcribed, and the corresponding cDNA was loaded into a 96-well plate provided by the manufacturer that contains PCR primers of the rat apoptotic genes. 3D profile graph shows the fold difference in the expression of each gene in MCAO-subjected ischemic rat brain samples vs. sham controls. Columns pointing up (with *z*-axis values >1) indicate up-regulation of gene expression, and columns pointing down (with *z*-axis values <1) indicate down-regulation of gene expression. Corresponding scatter plots show the validity of the experiment and the expression level of each gene in MCAO-subjected vs. sham control samples; $n \geq 3$

Apoptosis Antibody Array

Cell lysates obtained from the brain tissue of sham control rats and the ipsilateral ischemic brain tissue of rats that were sacrificed 7 days post-MCAO procedure were subjected to human apoptosis antibody array (Ray Biotech, Norcross, GA). Based on the manufacturer's inputs, several of these antibodies used in the preparation of the human apoptosis antibody array have cross reactivity with rat apoptotic proteins. The array membranes obtained were processed as per the manufacturer's instructions. Data were analyzed using ImageJ analysis software.

Immunoblot Analysis

Immunoblot analysis was performed to check the expression of various proteins in tissue lysates of untreated and treated ischemic brains and the respective brain tissues of sham controls. After sacrificing the animals at the end of the study, their brains were rapidly removed and frozen at −70 °C. Appropriate portions of the tissue were resuspended in 0.2 ml of homogenization buffer (250 mM sucrose, 10 mM HEPES, 10 mM Tris–HCl, 10 mM KCl, 1 % NP-40, 1 mM NaF, 1 mM Na_3VO_4, 1 mM EDTA, 1 mM DTT, 0.5 mM PMSF plus protease inhibitors [1 μg/ml pepstatin, 10 μg/ml leupeptin and 10 μg/ml aprotinin]; pH 7.4), homogenized using a Tissue Tearor (Biospec Products, Inc.), and followed by sonication. Tissue homogenate was centrifuged at $15,000 \times g$ for 30 min at 4 °C and the protein levels in the supernatant were determined using the BCA assay (Pierce, Rockford, IL). Samples [equal amount (30–80 μg) of total protein/well] were subjected to 10–14 % SDS-PAGE based on the specifications of the protein, and the protein bands on the gel were transferred onto nitrocellulose membranes. The membranes were processed with primary antibodies followed by appropriate HRP-conjugated secondary antibodies. Immunoreactive bands were visualized using chemiluminescence ECL Western blotting detection reagents on Hyperfilm-MP autoradiography film (Amersham, Piscataway, NJ). Immunoblots were reprobed and processed with GAPDH antibody to verify that similar amounts of protein were loaded in all lanes.

Statistical Analysis

Statistical comparisons were performed using Graph Pad Prism software (version 3.02). Quantitative data from TTC staining, TUNEL assay, and caspase-3 immunofluorescence were evaluated for statistical significance using one-way ANOVA. Bonferroni's post hoc test (multiple comparison tests) was used to compare any statistical significance among the groups. Differences in the values were considered significant at $p < 0.05$.

Results

Brain Damage After Focal Cerebral Ischemia

TTC staining performed to evaluate the infarct size in animals subjected to either 1 or 2 h MCAO, which were sacrificed on either day 1 or day 7 post-MCAO procedure, revealed a prominent and comparable infarct size in rats subjected to 2 h MCAO procedure and sacrificed on day 1 or day 7 post-MCAO (Fig. 1a). Infarct size was significantly less in animals subjected to 1 h MCAO compared to those subjected to 2 h MCAO (Fig. 1b). Although there was a slight reduction in infarct size in animals subjected to 2 h MCAO and 7 days reperfusion as compared with those subjected to 2 h MCAO and 1 day reperfusion, the difference was not statistically significant. As expected, no infarction was noticed in the coronal brain sections of sham-operated animals and in the contralateral regions of MCAO-subjected rat brains. Based on these results, it was decided to induce ischemia for a period of 2 h in subsequent experiments designed to evaluate apoptosis.

In addition, the H&E staining on sham-operated and 2 h MCAO-subjected animals sacrificed at various time points after reperfusion (PSD1, PSD3, PSD5 and PSD7) revealed prominent structural brain damage in the ischemic regions with increasing intensity from PSD1 through PSD7 (Fig. 2). Respective magnified images of the cortex and striatal regions of the ischemic core showed interstitial edema and pyknotic nuclei that were absent in controls. In contrast to TTC staining results, H&E staining of MCAO-subjected rats clearly demonstrated the extent of structural damage in the ischemic brain regions, which prominently increased with the increase in reperfusion time.

Table 3 Regulation of apoptotic genes involved in the induction and positive regulation of apoptosis after focal cerebral ischemia and reperfusion in rats

Gene	Reference sequence	Fold up- or down-regulation	
		2 h MCAO+1 day Reperfusion vs. control	2 h MCAO+7 days Reperfusion vs. control
Bad	NM_022698	1.14	**3.50***
Bak1	NM_053812	1.86	**7.00***
Bax	NM_017059	1.81	**6.48***
Bcl2l11 (Bim)	NM_022612	−1.05	**6.26***
Bcl10	NM_031328	1.59	**4.86**
Bid	NM_022684	1.79	**8.65***
Bik	NM_053704	1.50	**8.65**
Bok	NM_017312	1.40	**4.03***
Caspase 1 (Ice)	NM_012762	1.22	**5.19**
Caspase 12	NM_130422	1.24	**5.34**
Caspase 14	XM_234878	**3.88**	**9.25**
Caspase 2	NM_022522	1.35	**7.48**
Caspase 3	NM_012922	1.77	**6.26**
Caspase 4	NM_053736	1.24	**4.51**
Caspase 6	NM_031775	1.57	**8.32***
Caspase 7	NM_022260	**2.01**	**9.76***
Caspase 8	NM_022277	1.27	**8.40***
Caspase 8ap2	NM_001107921	−1.12	**4.20**
Cd40	NM_134360	1.65	**9.17***
Cidea	NM_001170467	1.45	**10.73**
Cideb	NM_001108869	**4.41**	**8.92***
Dapk1	NM_001107335	1.85	**6.19***
Dffa	NM_053679	1.72	**7.98**
Dffb (Cad)	NM_053362	1.98	**11.08**
Diablo (Smac)	NM_001008292	1.38	**5.16***
Fadd	NM_152937	1.91	**10.6***
Fasl (CD95-L)	NM_012908	1.12	**7.16**
Gadd45a	NM_024127	**2.96**	**4.13***
Hrk	NM_057130	−1.02	**3.51***
Lta (Tnfb)	NM_080769	1.36	**7.59***
Ltbr	NM_001008315	**2.39**	**6.36***
Mapk1 (Erk2)	NM_053842	1.02	**3.70**
Pycard (Tms1/Asc)	NM_172322	1.60	**8.46***
Ripk2	XM_342810	1.47	**5.28**
Tnfrsf10b	NM_001108873	**6.10***	1.52
Tnfrsf11b	NM_012870	1.61	**6.28**
Tnfrsf1a (Tnfr1)	NM_013091	**3.04**	**6.44***
Tnfrsf1b (Tnfr2)	NM_130426	1.42	**9.21***
Tnfsf10 (Trail)	NM_145681	−1.05	**7.43**
Tnfsf12	NM_001001513	1.79	**6.79***
Tp53 (p53)	NM_030989	**2.16**	**4.09**
Tp63	NM_019221	1.70	**9.72**
Tradd	NM_001100480	1.60	**6.88***
Traf3	NM_001108724	1.59	**6.50**

Fold up- or down- regulation values which are greater or less than 2 are indicated in *bold*

*$p<0.05$

Table 4 Regulation of apoptotic genes involved in the inhibition and negative regulation of apoptosis after focal cerebral ischemia and reperfusion in rats

Gene	Reference sequence	Fold up- or down-regulation	
		2 h MCAO+1 day Reperfusion vs. control	2 h MCAO+7 days Reperfusion vs. control
Annexin A5 (Anxa5)	NM_013132	1.79	**3.69***
Api5	NM_001127379	1.52	**3.42**
Aven	NM_001107757	1.04	**4.18***
Bcl2	NM_016993	1.47	**7.03***
Bcl2a1d	NM_133416	1.54	**6.15**
Bcl2l1 (Bcl-x)	NM_031535	1.79	**6.51***
Bcl2l2	NM_021850	1.63	**6.08**
Birc2 (c-IAP2)	NM_021752	1.58	**3.84**
Birc3 (c-IAP1)	NM_023987	1.83	**9.56**
Birc4 (XIAP)	NM_022231	**−2.13**	**3.44**
Birc5 (Survivin)	NM_022274	1.36	**7.73***
Bnip2	NM_001106835	1.55	**6.08***
Card10	NM_001130554	1.43	**7.11***
Cd40lg (Tnfsf5)	NM_053353	**−2.86**	**7.45**
Faim	NM_080895	1.19	**3.65**
Il10	NM_012854	1.29	**8.77***
Mcl1	NM_021846	1.71	**3.39**
Naip2	XM_226742	1.01	**9.32***
Nol3	NM_053516	1.47	**5.66***
Polb	NM_017141	1.23	**4.53**
Prlr	NM_012630	**2.85**	**7.06**
Sphk2	NM_001012066	1.38	**4.38**

Fold up- or down-regulation values which are greater or less than 2 are indicated in *bold*

*$p < 0.05$

Apoptosis After MCAO and Reperfusion

TUNEL-positive/apoptotic cells were identified in the ischemic brain regions of all groups of animals subjected to MCAO followed by various periods of reperfusion (Fig. 3a). A minimum of 60 % of TUNEL-positive cells were present in the ipsilateral brain regions of all animals, irrespective of the reperfusion time (Fig. 3b). The highest number of TUNEL-positive cells was noticed in ischemic brain sections of animals that were reperfused for 7 days after MCAO. The absence of TUNEL-positive cells in the respective contralateral brain regions indicated that the apoptosis was specific to ischemic brain regions.

Apoptosis was also demonstrated by immunofluorescence analysis which revealed prominent protein expression of caspase-3 in all the groups of animals subjected to MCAO followed by various periods of reperfusion (Fig. 3c). As expected, caspase-3 protein expression is absent in the respective contralateral regions. Caspase-dependent apoptosis was significantly greater in animals subjected a minimum of 3 days of reperfusion compared to those subjected to 1 day reperfusion (Fig. 3d).

Finally, neuronal apoptosis was indicated by prominent colocalization of caspase-3 protein expression with NeuN in various regions of the ischemic core and the penumbra in animals subjected to 7 days of reperfusion (Fig. 4a). Although

Table 5 Regulation of apoptotic genes that can either induce or inhibit apoptosis after focal cerebral ischemia and reperfusion in rats

Gene	Reference sequence	Fold up- or down-regulation	
		2 h MCAO+1 day Reperfusion vs. control	2 h MCAO+7 days Reperfusion vs. control
Akt1	NM_033230	1.65	**3.47***
Cflar (Casper) (Flip)	NM_057138	1.47	**4.45**
NF-kB (Nfkb1) (p50)	XM_342346	**2.23**	8.06*
Tnf	NM_012675	1.42	**7.59***
Tp73	NM_001108696	**5.86**	**10.44**

Fold up- or down-regulation values which are greater or less than 2 are indicated in *bold*

*$p < 0.05$

it had previously been shown that necrosis occurs in ischemic core, our findings indicate that certain neurons still expressed NeuN; these NeuN positive neurons also showed prominent caspase-3 expression, indicating that these cells are in the process of undergoing apoptosis.

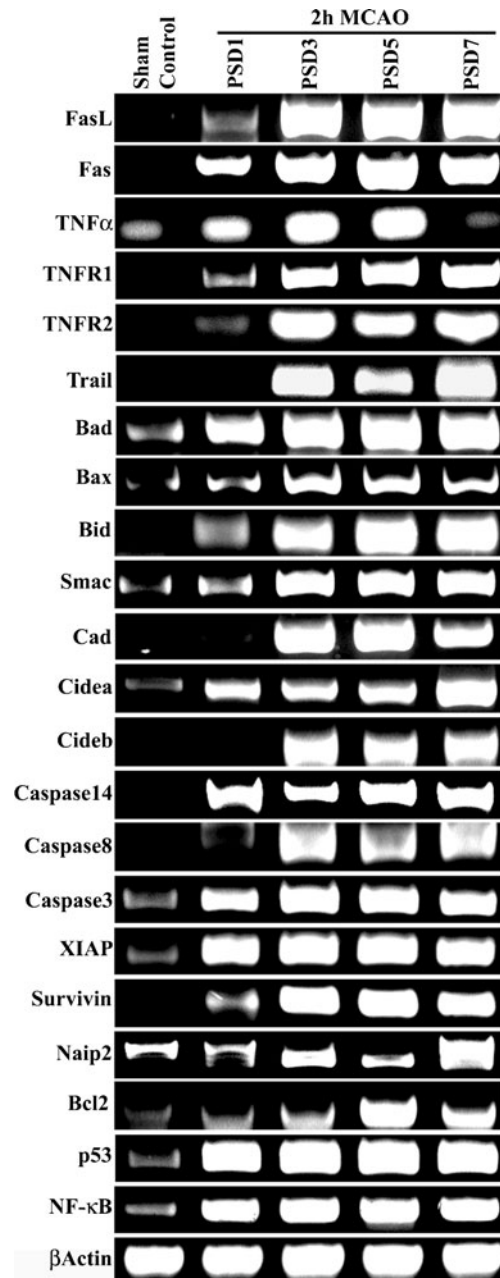## Regulation of Apoptotic Molecules After Focal Cerebral Ischemia

Rat apoptotic PCR microarray analysis results indicated up-regulation of relatively few apoptotic genes in the samples obtained from animals subjected to 1 day reperfusion after MCAO. Conversely, animals subjected to 7 days reperfusion after MCAO demonstrated an up-regulation of 90 % of the apoptotic genes (Fig. 4b). Interestingly, we also noticed increased gene expression of inhibitors of apoptosis, such as Birc2, Birc3, XIAP, survivin, Naip2, AnnexinA5, and Bcl2, in animals subjected to 7 days reperfusion after MCAO. The increased gene expression of anti-apoptotic molecules could be attributed to the activation of the body's defense mechanism to fight against increased apoptosis.

Folds up- or down-regulation of various apoptotic and anti-apoptotic molecules at mRNA level are presented in Tables 3, 4, and 5. Increased mRNA expression of certain apoptotic and anti-apoptotic genes (FasL, Fas, TNFR1, TNFR2, bad, bax, bid, smac, cidea, caspase-14, caspase-3, XIAP, survivin, bcl-2, p53 and NFkb1) appears to have been initiated on day 1 post-MCAO with increasing expression through 7 days post-MCAO (Fig. 5). However, prominent mRNA expression of certain molecules such as Trail, cad, cideb, caspase-8 and naip2 was noticed only in three days post-MCAO samples, and then the expression of these molecules remained elevated for 7 days.

To further evaluate these results, we conducted an apoptosis antibody array with the cell lysates obtained from the brain tissue of sham control rats and the ipsilateral ischemic brain tissue of rats subjected to 7 days reperfusion. Brain tissues of sham-operated animals were used as controls instead of contralateral brain tissues of MCAO-induced animals because the induction of ischemia in a whole animal may lead to induction/inhibition of the expression of certain proteins in other regions of the brain. Therefore, the protein expression profile in the contralateral brain region may not exactly represent the normal brain and may lead to false interpretations.

As expected, MCAO animals status post 7 day reperfusion, but not sham animals, demonstrated prominent protein expression of several apoptotic and anti-apoptotic molecules (bad, bax, bcl-2, bcl-w, bid, bim, caspase-3, caspase-8, IAP-2, cytochrome c, Fas, FasL, HSP27, HSP60, HSP70, HTRA, p21, p27, p53, smac, survivin, TNFR1, TNFR2, TNF-alpha, and XIAP) (Fig. 6a).

Finally, we also conducted immunoblot analysis on tissue samples obtained from sham-operated and 2-h MCAO-subjected animals that were reperfused for several time periods. Immunoblot analysis revealed an interesting protein expression profile of various apoptotic molecules that varies across the

Fig. 5 Temporal regulation of various apoptotic and anti-apoptotic molecules at the mRNA level after focal middle cerebral artery occlusion (MCAO) in rats. RT-PCR analysis was performed following a standard protocol on cDNAs obtained from the brains of sham-operated animals and the ischemic brain regions of MCAO-subjected rats sacrificed at various time points after reperfusion (PSD1, PSD3, PSD5 and PSD7). Agarose gel electrophoresis conducted on the samples obtained after RT-PCR analysis depicts the expression profile of various apoptotic and anti-apoptotic molecules at the mRNA level; $n \geq 3$. β-Actin was used as a loading control
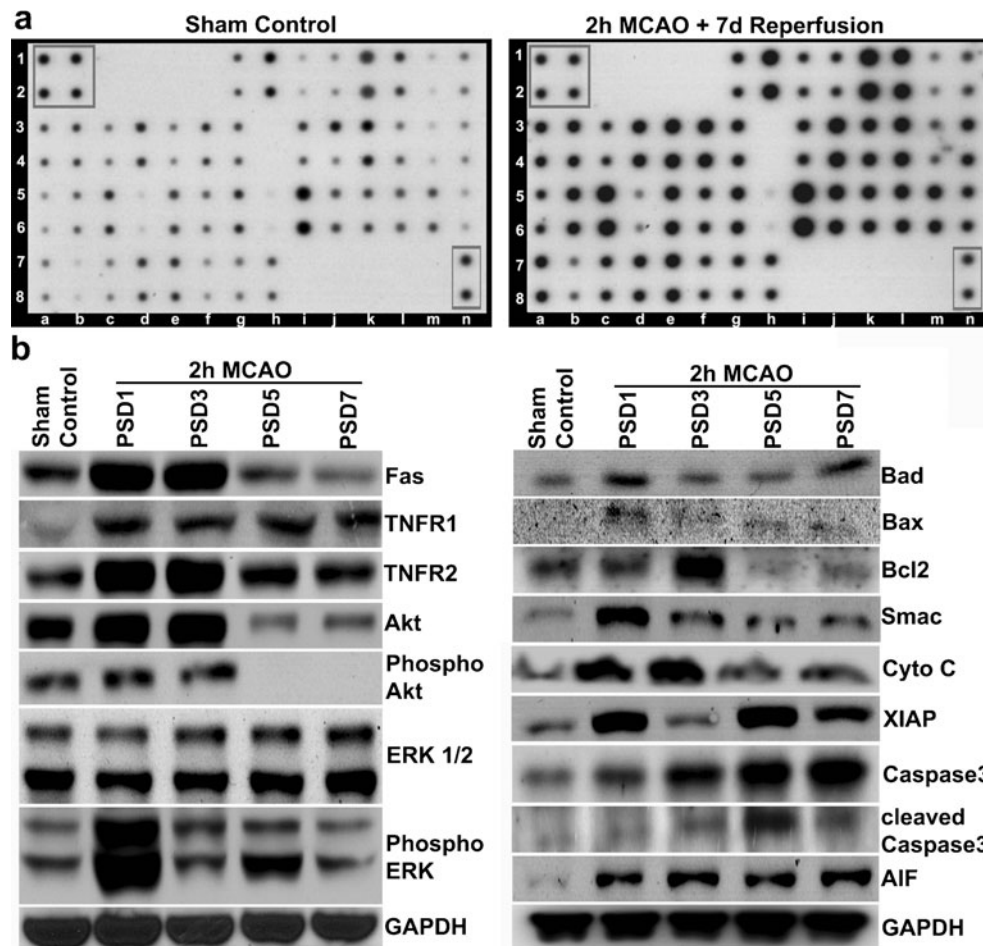
Fig. 6 Protein expression profile of various apoptotic molecules after focal middle cerebral artery occlusion (*MCAO*) in rats. **a** Brain tissue lysates from sham-operated and 2 h MCAO-subjected rats sacrificed 7 days post-MCAO were subjected to apoptotic antibody array as per the manufacturer's instructions. Results shown are representative of three independent experiments. Array membranes were subjected to various tissue lysates obtained from rat brains of various groups containing equal amounts of protein. *Highlighted portions* on the arrays (a1, a2, b1, b2, n1 and n2) represent positive controls. Protein expression of several apoptotic and anti-apoptotic molecules such as bad (g1, g2), bax (h1, h2), bcl-2 (i1, i2), bcl-w (j1, j2), BID (k1, k2), BIM (l1, l2), caspase-3 (m1, m2), caspase-8 (n1, n2), cIAP-2 (b3, b4), cytochrome *c*

(d3, d4), Fas (f3, f4), FasL (g3, g4), HSP27 (i3, i4), HSP60 (j3, j4), HSP70 (k3, k4), HTRA (l3, l4), livin (h5, h6), p21 (i5, i6), p27 (j5, j6), p53 (k5, k6), SMAC (l5, l6), survivin (m5, m6), TNFR1 (n5, n6), TNFR2 (a7, a8), TNF-alpha (b7, b8) and XIAP (h7, h8) was prominently increased after focal cerebral ischemia followed by reperfusion. **b** Immunoblot analysis was performed following a standard protocol on tissue lysates obtained from the brains of sham-operated animals and the ischemic brain regions of MCAO-subjected rats sacrificed at various time points after reperfusion (PSD1, PSD3, PSD5, and PSD7). Immunoblots depicts the protein expression profile of various apoptotic and anti-apoptotic molecules; $n \geq 3$. GAPDH was used as a loading control

samples (Fig. 6b). Prominent protein expression of Fas, TNFR2, Akt and cytochrome *c* was noticed in animals subjected to 1 and 3 days of reperfusion compared to other samples. Similarly, a prominent protein expression of phospho-ERK, bad, bax, Smac, and XIAP was noticed in animals subjected to 1 day reperfusion. XIAP expression was prominent also in animals subjected to 5 and 7 days of reperfusion. Caspase-3 protein expression was prominent in MCAO-subjected animals compared to sham-operated animals, and the expression gradually increased from day 1 through day 7 reperfusion times. Expression of cleaved caspase-3 was seen in samples of animals subjected to 3, 5 and 7 days reperfusion.

Discussion

Cerebral ischemia and reperfusion injury triggers multiple and distinct but overlapping cell signaling pathways, which may lead to cell damage or cell survival. There is overwhelming evidence to suggest that in addition to necrosis, apoptosis contributes significantly to cell death both in the ischemic core and in the surrounding penumbra region subsequent to cerebral ischemia and reperfusion. The ischemic penumbra will have intermediate perfusion, where cells depolarize intermittently [16–18]. Without treatment, the penumbra often progresses to infarction.

Many susceptible neurons, particularly in the penumbra region, undergo apoptosis, although the mechanisms of this process are not fully understood [19, 20]. Both extrinsic and intrinsic (also known as the mitochondrial pathway) apoptotic pathways play vital roles, and upon initiation, these pathways recruit downstream apoptotic molecules to trigger cell death [21]. Each of these pathways contains both caspase-dependent and caspase-independent components. Apoptotic PCR and antibody arrays performed in the current study clearly demonstrated the expression profiles of various apoptotic molecules at various stages after focal cerebral ischemia both at mRNA and protein levels.

The brain also activates neuroprotective mechanisms in an attempt to counteract the damaging effects after cerebral ischemia and reperfusion. This was confirmed in this study wherein increased expression of the anti-apoptotic molecules, such as Akt, ERK1/2, Phospho-ERK, Bcl2, IAP, XIAP, Naip2, survivin, livin, HSP27, HSP60, and HSP70, was demonstrated. Although there was an up-regulation of Akt at mRNA levels 7 days after reperfusion compared to its mRNA level on 1 day after reperfusion, the protein expressions of Akt and phospho-Akt were prominently decreased 5 days after reperfusion (Table 5; Fig. 6b). Similarly, the protein expression of phospho-ERK was more prominent on 1 day after reperfusion than at any other time point (Fig. 6b). Interestingly, the activation of ERK1/2 also has been shown to contribute to cell death in animal models of ischemia-induced brain injury [22, 23]. This would suggest that ERK1/2 is associated with both brain injury and anti-apoptosis.

Earlier investigations revealed that liposome-mediated, site-specific delivery of a plasmid encoding human Bcl-2 protein significantly reduced the number of apoptotic cells in the infarct and the penumbra area after MCAO in rats [24]. A well-recognized property of the highly conserved inhibitor of apoptosis protein (IAP) gene family is the ability to prevent apoptosis. So far, in humans, the members of the IAP family include cIAP1, cIAP2, XIAP, NAIP (neuronal apoptosis inhibitory protein), survivin, and livin. In the present study, the expression of the above-listed members of the IAP family increased prominently following focal cerebral ischemia. We noticed several fold up-regulation of XIAP, survivin, Naip2, cIAP1 and cIAP2 mRNA levels 7 days after reperfusion compared to their levels 1 day after reperfusion (Table 4). Similar to their mRNA levels, the protein expressions of these molecules were also prominent 7 days after reperfusion compared to their expression in sham-operated animals (Fig. 6a). Unlike Naip2, the mRNA expressions of XIAP and survivin 1 day after reperfusion were prominent compared to their mRNA expressions in sham-operated animals (Fig. 5). XIAP protein expression was increased 1 day after reperfusion compared to sham-operated animals, and the increased expression was maintained 5 and 7 days after reperfusion (Fig. 6b). Adenovirus-mediated overexpression

of XIAP inhibits cell death in the substantia nigra and cerebellar granules [25, 26].

Overexpression of HSP70 sequesters apoptosis-inducing factor (AIF) and protects the neonatal brain subjected to hypoxia–ischemic brain injury [27]. Although we are not yet clear about the mechanisms underlying AIF-induced apoptosis after focal cerebral ischemia, AIF protein expression was prominent in the samples subjected to MCAO, and its expression levels were maintained from day 1 through day 7 of reperfusion (Fig. 6b).

The increased expression of both pro-apoptotic and anti-apoptotic molecules after focal cerebral ischemia in the present study is in agreement with earlier reports [7, 21, 28]. The current study also details the temporal distribution of the mRNA and protein expression of these molecules at various stages of reperfusion after ischemia.

Bax, Bad, and Bid form channels allowing the release of cytochrome c from the mitochondrial inter-membrane space. Release of cytochrome c is the main trigger for mitochondrial-associated apoptosis [29–31]. Cytochrome c induces oligomerization of APAF-1, subsequent binding with pro-caspase-9, activation of caspase-9, and finally binding and activation of caspase-3, which cleaves PARP and initiates apoptosis [12, 30]. In the present study, we noticed an increased mRNA and protein expression levels of Bax, Bad, Bid, and caspase-3 within 24 h following reperfusion (Figs. 5 and 6b). We also noticed a prominent increase in the expression of cytochrome c within the same time period, and the expression remained elevated until 72 h post reperfusion (Fig. 6b). Unlike the mRNA expressions of Bax and Bad which remained elevated until 7 days post-reperfusion, their protein expressions were prominently decreased 3 days post-reperfusion compared to their expressions 1 day post-reperfusion (Figs. 5 and 6b). Caspase 3 protein expression increased from day 1 through day 7 post-reperfusion (Fig. 6b). Cleaved caspase-3 expression noticed after 72 h of reperfusion in the current study clearly indicated the presence of caspase-dependent component of the intrinsic (mitochondrial) apoptotic pathway.

Earlier investigations using broad-spectrum caspase inhibitors, like zVADfmk, BAF, or zDEVDfmk, have demonstrated these to be neuroprotective in animal models of focal and global cerebral ischemia, and neonatal hypoxic–ischemic brain injury [8–11, 32]. A cocktail of caspase inhibitors (e.g., YVADcmk, DEVDfmk, and IETDfmk) has been shown to reduce the number of apoptotic cells after MCAO in rats [12]. In addition, IDN-6556 is a broad-spectrum caspase inhibitor and when administered during phase II clinical trials, offered local therapeutic protection against cold ischemia/warm reperfusion-mediated apoptosis and injury [15]. Non-caspase-mediated induction of apoptosis by the intrinsic apoptotic pathway after stroke, which involves mitochondrial release of AIF and subsequent DNA fragmentation, has also been described, but the exact mechanisms have yet to be defined [33, 34].

Release of TNF-α by neurons and glia [35–37] and up-regulation of Fas mRNA and protein levels have been observed in the vulnerable areas after hypoxic ischemic injury. Released pro-inflammatory cytokines, such as TNF-α and IL-1, activate a number of intracellular signaling pathways, which results in neuronal apoptosis. Caspase-dependent neuronal apoptosis in the ischemic core regions and the penumbra was clearly demonstrated in the current study (Fig. 4a). TNF-α activates TNF-receptor-associated death domain (TRADD), while Fas ligand, which is secreted by the action of matrix metalloproteinases, associates with Fas-associated death domain (FADD). Subsequently, the death domains of these proteins interact with the death effector domains of procaspase-8, cleaving it, and in turn, activating downstream effector caspases and apoptosis [38, 39]. Furthermore, a marked increase in the Fas-L expression was found in the penumbral region during early reperfusion after MCAO [31]. The current study supports this assertion, as we found prominent increases in the mRNA and protein expression of TNF-α, FasL, Fas, TNFR1 and TNFR2 within 24 h after reperfusion (Figs. 5 and 6b). The increased mRNA expression of FasL, Fas, TNFR1 and TNFR2 remained elevated or further increased until 7 days post-reperfusion. Similar to mRNA expression, the increased protein expression of TNFR1 remained elevated until 7 days after reperfusion. However, the increased protein expression of Fas and TNFR2 remained elevated until 3 days post-reperfusion and decreased thereafter. In addition, we also noticed an increase in mRNA levels of FADD and TRADD within 24 h after reperfusion, and this increase was statistically significant in samples that were analyzed 7 days after reperfusion (Table 3). Furthermore, BH3-only death-promoting factor, Bid, is involved in TNF/Fas family death receptor-mediated extrinsic pathway. Activated caspase-8 leads to the cleavage of Bid to activated form, tBid. Then, tBid targets the mitochondrial membrane, and through conformational changes in Bax, it triggers cytochrome c release that may finally lead to activation of caspase-3 [40, 41]. In the present study, mRNA expression of Bid increased within 24 h after reperfusion, and this increased expression was sustained until 7 days after reperfusion (Fig. 5; Table 3). Similar to mRNA expression/level, protein expression of Bid was also prominent 7 days post-reperfusion compared to its expression in sham-operated animals (Fig. 6a).

In summary, our study provides a broad survey of pro-apoptotic and anti-apoptotic molecules and their temporal expression profiles both at the transcriptional and translational levels. This data is very important for designing future stroke therapies, particularly those that target apoptosis. The main strategies in stroke treatment targeting apoptosis should include either silencing key apoptotic molecules or overexpression of anti-apoptotic molecules. Several of the reported anti-apoptotic therapies to date targeted only the molecules of the intrinsic apoptotic pathway. Furthermore,

these studies targeted a single molecule/mechanism, which may not provide the desired therapeutic benefit due to the complex pathology of the ischemic stroke. Because of the apoptotic cross-talk among several pathways, inhibition of one apoptotic pathway may augment an alternative one. It is crucial that neuroprotective approaches to treat cerebral ischemia should include combination treatment strategies for optimal clinical outcomes. Furthermore, to succeed in clinical settings, future stroke treatments should consider the specificity, timing, and frequency of the treatment and should also target the appropriate key molecules or pathways. We strongly believe that our study provides invaluable data for investigators working in this area to design effective stroke therapies in the future.

References

1. Banerjee S, Williamson D, Habib N, Gordon M, Chataway J (2011) Human stem cell therapy in ischaemic stroke: a review. Age Ageing 40:7–13
2. Ferrer I (2006) Apoptosis: future targets for neuroprotective strategies. Cerebrovasc Dis 21(Suppl 2):9–20
3. Benchoua A, Guegan C, Couriaud C, Hosseini H, Sampaio N, Morin D, Onteniente B (2001) Specific caspase pathways are activated in the two stages of cerebral infarction. J Neurosci 21:7127–7134
4. Nicotera P, Leist M, Ferrando-May E (1998) Intracellular ATP, a switch in the decision between apoptosis and necrosis. Toxicol Lett 102–103:139–142
5. Schwab BL, Guerini D, Didszun C, Bano D, Ferrando-May E, Fava E, Tam J, Xu D, Xanthoudakis S, Nicholson DW et al (2002) Cleavage of plasma membrane calcium pumps by caspases: a link between apoptosis and necrosis. Cell Death Differ 9:818–831
6. Bano D, Young KW, Guerin CJ, Lefeuvre R, Rothwell NJ, Naldini L, Rizzuto R, Carafoli E, Nicotera P (2005) Cleavage of the plasma membrane Na$^+$/Ca^{2+} exchanger in excitotoxicity. Cell 120:275–285
7. Nakka VP, Gusain A, Mehta SL, Raghubir R (2008) Molecular mechanisms of apoptosis in cerebral ischemia: multiple neuroprotective opportunities. Mol Neurobiol 37:7–38
8. Loddick SA, MacKenzie A, Rothwell NJ (1996) An ICE inhibitor, z-VAD-DCB attenuates ischaemic brain damage in the rat. Neuroreport 7:1465–1468
9. Hara H, Friedlander RM, Gagliardini V, Ayata C, Fink K, Huang Z, Shimizu-Sasamata M, Yuan J, Moskowitz MA (1997) Inhibition of interleukin 1beta converting enzyme family proteases reduces ischemic and excitotoxic neuronal damage. Proc Natl Acad Sci USA 94:2007–2012
10. Endres M, Namura S, Shimizu-Sasamata M, Waeber C, Zhang L, Gomez-Isla T, Hyman BT, Moskowitz MA (1998) Attenuation of

delayed neuronal death after mild focal ischemia in mice by inhibition of the caspase family. J Cereb Blood Flow Metab 18:238–247

11. Cheng Y, Deshmukh M, D'Costa A, Demaro JA, Gidday JM, Shah A, Sun Y, Jacquin MF, Johnson EM, Holtzman DM (1998) Caspase inhibitor affords neuroprotection with delayed administration in a rat model of neonatal hypoxic–ischemic brain injury. J Clin Invest 101:1992–1999

12. Krupinski J, Lopez E, Marti E, Ferrer I (2000) Expression of caspases and their substrates in the rat model of focal cerebral ischemia. Neurobiol Dis 7:332–342

13. Mouw G, Zechel JL, Zhou Y, Lust WD, Selman WR, Ratcheson RA (2002) Caspase-9 inhibition after focal cerebral ischemia improves outcome following reversible focal ischemia. Metab Brain Dis 17:143–151

14. Fischer U, Schulze-Osthoff K (2005) Apoptosis-based therapies and drug targets. Cell Death Differ 12(Suppl 1):942–961

15. Baskin-Bey ES, Washburn K, Feng S, Oltersdorf T, Shapiro D, Huyghe M, Burgart L, Garrity-Park M, van Vilsteren FG, Oliver LK et al (2007) Clinical trial of the pan-caspase inhibitor, IDN-6556, in human liver preservation injury. Am J Transplant 7:218–225

16. Obrenovitch TP (1995) The ischaemic penumbra: twenty years on. Cerebrovasc Brain Metab Rev 7:297–323

17. Strong AJ, Smith SE, Whittington DJ, Meldrum BS, Parsons AA, Krupinski J, Hunter AJ, Patel S, Robertson C (2000) Factors influencing the frequency of fluorescence transients as markers of peri-infarct depolarizations in focal cerebral ischemia. Stroke 31:214–222

18. Phan TG, Wright PM, Markus R, Howells DW, Davis SM, Donnan GA (2002) Salvaging the ischaemic penumbra: more than just reperfusion? Clin Exp Pharmacol Physiol 29:1–10

19. MacManus JP, Buchan AM (2000) Apoptosis after experimental stroke: fact or fashion? J Neurotrauma 17:899–914

20. Zheng Z, Zhao H, Steinberg GK, Yenari MA (2003) Cellular and molecular events underlying ischemia-induced neuronal apoptosis. Drug News Perspect 16:497–503

21. Zhang F, Yin W, Chen J (2004) Apoptosis in cerebral ischemia: executional and regulatory signaling mechanisms. Neurol Res 26:835–845

22. Alessandrini A, Namura S, Moskowitz MA, Bonventre JV (1999) MEK1 protein kinase inhibition protects against damage resulting from focal cerebral ischemia. Proc Natl Acad Sci U S A 96:12866–12869

23. Zhuang S, Schnellmann RG (2006) A death-promoting role for extracellular signal-regulated kinase. J Pharmacol Exp Ther 319:991–997

24. Cao YJ, Shibata T, Rainov NG (2002) Liposome-mediated transfer of the bcl-2 gene results in neuroprotection after in vivo transient focal cerebral ischemia in an animal model. Gene Ther 9:415–419

25. Simons M, Beinroth S, Gleichmann M, Liston P, Korneluk RG, MacKenzie AE, Bahr M, Klockgether T, Robertson GS, Weller M et al (1999) Adenovirus-mediated gene transfer of inhibitors of apoptosis protein delays apoptosis in cerebellar granule neurons. J Neurochem 72:292–301

26. Eberhardt O, Coelln RV, Kugler S, Lindenau J, Rathke-Hartlieb S, Gerhardt E, Haid S, Isenmann S, Gravel C, Srinivasan A et al (2000) Protection by synergistic effects of adenovirus-mediated X-chromosome-linked inhibitor of apoptosis and glial cell line-derived neurotrophic factor gene transfer in the 1-methyl-4-phenyl-1,2,3,6-tetrahydropyridine model of Parkinson's disease. J Neurosci 20:9126–9134

27. Matsumori Y, Hong SM, Aoyama K, Fan Y, Kayama T, Sheldon RA, Vexler ZS, Ferriero DM, Weinstein PR, Liu J (2005) Hsp70 overexpression sequesters AIF and reduces neonatal hypoxic/ischemic brain injury. J Cereb Blood Flow Metab 25:899–910

28. Slevin M, Krupinski J, Kumar P, Gaffney J, Kumar S (2005) Gene activation and protein expression following ischaemic stroke: strategies towards neuroprotection. J Cell Mol Med 9:85–102

29. Fujimura M, Morita-Fujimura Y, Kawase M, Copin JC, Calagui B, Epstein CJ, Chan PH (1999) Manganese superoxide dismutase mediates the early release of mitochondrial cytochrome C and subsequent DNA fragmentation after permanent focal cerebral ischemia in mice. J Neurosci 19:3414–3422

30. Love S (2003) Apoptosis and brain ischaemia. Prog Neuro-psychopharmacol Biol Psychiatry 27:267–282

31. Ferrer I, Planas AM (2003) Signaling of cell death and cell survival following focal cerebral ischemia: life and death struggle in the penumbra. J Neuropathol Exp Neurol 62:329–339

32. Li H, Colbourne F, Sun P, Zhao Z, Buchan AM, Iadecola C (2000) Caspase inhibitors reduce neuronal injury after focal but not global cerebral ischemia in rats. Stroke 31:176–182

33. Zhan RZ, Wu C, Fujihara H, Taga K, Qi S, Naito M, Shimoji K (2001) Both caspase-dependent and caspase-independent pathways may be involved in hippocampal CA1 neuronal death because of loss of cytochrome c From mitochondria in a rat forebrain ischemia model. J Cereb Blood Flow Metab 21:529–540

34. Cregan SP, Dawson VL, Slack RS (2004) Role of AIF in caspase-dependent and caspase-independent cell death. Oncogene 23:2785–2796

35. Rupalla K, Allegrini PR, Sauer D, Wiessner C (1998) Time course of microglia activation and apoptosis in various brain regions after permanent focal cerebral ischemia in mice. Acta Neuropathol 96:172–178

36. Botchkina GI, Geimonen E, Bilof ML, Villarreal O, Tracey KJ (1999) Loss of NF-kappaB activity during cerebral ischemia and TNF cytotoxicity. Mol Med 5:372–381

37. Sairanen T, Carpen O, Karjalainen-Lindsberg ML, Paetau A, Turpeinen U, Kaste M, Lindsberg PJ (2001) Evolution of cerebral tumor necrosis factor-alpha production during human ischemic stroke. Stroke 32:1750–1758

38. Salvesen GS, Dixit VM (1999) Caspase activation: the induced-proximity model. Proc Natl Acad Sci USA 96:10964–10967

39. Thorburn A (2004) Death receptor-induced cell killing. Cell Signal 16:139–144

40. Li H, Zhu H, Xu CJ, Yuan J (1998) Cleavage of BID by caspase 8 mediates the mitochondrial damage in the Fas pathway of apoptosis. Cell 94:491–501

41. Luo X, Budihardjo I, Zou H, Slaughter C, Wang X (1998) Bid, a Bcl2 interacting protein, mediates cytochrome c release from mitochondria in response to activation of cell surface death receptors. Cell 94:481–490

Authors' contribution